Quantum Relaxation and Metastability of Lattice Bosons with Cavity-Induced Long-Range Interactions

Benjamin Blaß,[1,*] Heiko Rieger,[1,†] Gergő Roósz,[2,3,4,‡] and Ferenc Iglói[2,3,§]
[1]Theoretical Physics, Saarland University, D-66123 Saarbrücken, Germany
[2]Wigner Research Centre for Physics, Institute for Solid State Physics and Optics, H-1525 Budapest, P.O. Box 49, Hungary
[3]Institute of Theoretical Physics, Szeged University, H-6720 Szeged, Hungary
[4]Institute of Theoretical Physics, Technical University Dresden, D-01062 Dresden, Germany

(Received 29 November 2017; published 28 August 2018)

The coupling of cold atoms to the radiation field within a high-finesse optical resonator, an optical cavity, induces long-range interactions which can compete with an underlying optical lattice. The interplay between short- and long-range interactions gives rise to new phases of matter including supersolidity (SS) and density waves (DW), and interesting quantum dynamics. Here it is shown that for hard-core bosons in one dimension the ground state phase diagram and the quantum relaxation after sudden quenches can be calculated exactly in the thermodynamic limit. Remanent DW order is observed for quenches from a DW ground state into the superfluid (SF) phase below a dynamical transition line. After sufficiently strong SF to DW quenches beyond a static metastability line DW order emerges on top of remanent SF order, giving rise to a dynamically generated SS state. Our method to handle infinite- and short-range interactions in the infinite system size limit opens a way to solve exactly other Hamiltonians with infinite- and short-range interactions as well.

DOI: 10.1103/PhysRevLett.121.095301

Cold atoms offer a broad range of possibilities to investigate properties of strongly interacting quantum many-body systems [1]. Bosonic particles in optical lattices [2] became a standard experimental tool to simulate the quantum mechanics of the Bose-Hubbard (BH) model [3], a paradigmatic theoretical model displaying Mott-insulating (MI) and superfluid (SF) phases [4]. In most experiments implementing an optical lattice the atoms have only short-range interactions, but it is known that longer-range interactions lead to new phases, like supersolids (SS) and density waves (DW), and interesting dynamics [5,6]. One way to extend the interaction range is to couple the atoms to an optical cavity, which can propagate interactions between atoms, making them effectively long ranged [7]. In combination with an optical lattice [8], recently an experimental setup was established [9] in which short- and long-range interactions compete and DW and SS phases occur. Subsequent theoretical studies using mean field theory [10–14] and Monte Carlo simulations [15] supported these findings. However, the quantum dynamics of the cold atoms in the optical cavity combined with an optical lattice is still elusive.

A widely used setup to study experimentally and theoretically the nonequilibrium dynamics of a closed many body quantum system is a sudden quench, in which a system is prepared in its ground state and system parameters are rapidly set to new values [16]. The central question addresses the nature of the system's stationary state after a long time evolution under its deterministic quantum dynamics. Nonintegrable systems are expected to evolve into a thermalized state, in which local observables can be characterized by thermal expectation values [17–27], whereas integrable systems develop into a state described by a generalized Gibbs ensemble [28–36]. Sudden quenches have been studied for bosons in optical lattices experimentally [37] and theoretically [38]. The underlying Hamiltonian, the BH model, is known to be nonintegrable, and thus the dynamics expected to thermalize, but numerical studies, comprising DMRG in one dimension [39], t-VMC in higher dimensions [40], or numerical dynamical MFT [41] indicate nonthermal behavior for certain strong quenches.

In this Letter we analyze the effect of cavity-induced interactions on the dynamics of bosons in an optical lattice. We show that for hard-core bosons (i.e., strong on-site repulsion allowing only single-particle occupancy) in one dimension the ground state phase diagram and the quantum relaxation after sudden quenches can be calculated exactly in the thermodynamic limit. In general, the presence of long-range interactions renders this system nonintegrable, but the cavity-induced interactions have a special form that allow for an analytical solution. We first determine the resulting ground state phase diagram comprising MI, DW, and SF phases, and then study the quantum relaxation after sudden quenches starting with DW and SF ground states, which give rise to dynamical phase transitions. Although the ground state phase diagram does not display a SS phase we will show that nonequilibrium states with simultaneous (time-averaged) DW and SF order do exist.

Bosons in an optical lattice with cavity-induced long-range interactions are described by an extended BH model [42,43]. As in the experimental setup of Ref. [9] we

consider the case in which the lattice constant of the optical lattice is half the wavelength of the cavity mode. Then the Hamiltonian is given by [9]

$$\hat{H} = -\mathcal{T}\sum_{\langle \mathbf{r},\mathbf{r}'\rangle}(\hat{b}^\dagger_{\mathbf{r}}\hat{b}_{\mathbf{r}'} + \text{H.c.}) + \frac{U}{2}\sum_{\mathbf{r}}\hat{n}_{\mathbf{r}}(\hat{n}_{\mathbf{r}} - 1) - \mu\sum_{\mathbf{r}}\hat{n}_{\mathbf{r}} - \varepsilon\frac{1}{N}\left(\sum\nolimits_{\mathbf{r}\in e}\hat{n}_{\mathbf{r}} - \sum\nolimits_{\mathbf{r}\in o}\hat{n}_{\mathbf{r}}\right)^2, \quad (1)$$

where $\hat{b}^\dagger_{\mathbf{r}}$ ($\hat{b}_{\mathbf{r}}$) are the Bose creation (annihilation) operators, $\hat{n}_{\mathbf{r}} = \hat{b}^\dagger_{\mathbf{r}}\hat{b}_{\mathbf{r}}$ the number operators, N the lattice size, $\mathcal{T}$ the tunneling constant, U the on-site repulsion, μ the chemical potential, and ε the strength of the infinite-range interactions induced by the cavity. The cavity-induced long-range interactions are represented as the square of the density wave order parameter $\hat{x}$,

$$\hat{x} = \frac{1}{N}\left(\sum_{\mathbf{r}\in e}\hat{n}_{\mathbf{r}} - \sum_{\mathbf{r}\in o}\hat{n}_{\mathbf{r}}\right), \quad (2)$$

where e and o stand for even and odd lattice sizes, respectively. Within the path integral representation of the partition function this square appears in the exponent and can thus be linearized by performing a Hubbard-Stratonovic transformation, introducing an auxiliary field. In the thermodynamic limit $N \to \infty$ this auxiliary field can be integrated out by a saddle point integration [44] yielding the effective Hamiltonian $H(x)$ in which the term $-\varepsilon N\hat{x}^2$ in Eq. (1) is replaced by $-2\varepsilon N x\hat{x} + \varepsilon N x^2$, with x the value of the auxiliary field at the saddle point given by the self-consistency equation

$$x = \langle\hat{x}\rangle_{\text{GS}[\hat{H}(x)]}, \quad (3)$$

the ground state expectation value of the imbalance. The equivalence of the two Hamiltonians $\hat{H}$ and $\hat{H}(x)$ with Eq. (3) is valid for bipartite lattices in arbitrary dimensions in the thermodynamic limit $N \to \infty$.

We consider the large U limit, excluding multiple site occupancies, in one dimension (experimentally realizable by a modification of the setup of Ref. [9], see discussion below). The Hamiltonian for a system of length L is thus given by

$$\hat{H}(x) = -\mathcal{T}\sum_{j=1}^{L}(\hat{a}^\dagger_j\hat{a}_{j+1} + \hat{a}_j\hat{a}^\dagger_{j+1}) + \varepsilon L x^2 - \sum_{j\text{even}}(\mu + 2\varepsilon x)\hat{a}^\dagger_j\hat{a}_j - \sum_{j\text{odd}}(\mu - 2\varepsilon x)\hat{a}^\dagger_j\hat{a}_j \quad (4)$$

and can be solved analytically. $\hat{a}^\dagger_j$ ($\hat{a}_j$) are the hard-core Bose creation (annihilation) operators. A Jordan-Wigner transformation followed by a Fourier transformation takes the Hamiltonian to the fermionic form

$$\hat{H}(x) = -\sum_{k>0}(c^\dagger_k, c^\dagger_{k-\pi})\begin{pmatrix}\alpha_k & \gamma_k\\ \gamma_k & \beta_k\end{pmatrix}\begin{pmatrix}c_k\\ c_{k-\pi}\end{pmatrix} + 2\varepsilon x^2, \quad (5)$$

with $k = (2n-1)\pi/L$, $n = 1,2,\ldots,L/2$, $\alpha_k = \mu + 2\mathcal{T}\cos(k)$, $\beta_k = \mu - 2\mathcal{T}\cos(k)$, and $\gamma = 2\varepsilon x$. The k and $k-\pi$ modes can be decoupled by a canonical transformation diagonalizing the Hamiltonian $\hat{H}(x) = \sum_{0<k<\pi/2} 2[\Lambda_k\hat{\eta}^\dagger_k\hat{\eta}_k + \Lambda_{k-\pi}\hat{\eta}^\dagger_{k-\pi}\hat{\eta}_{k-\pi} + 2\varepsilon x^2]$. The energies of the eigenmodes are $\Lambda_k = -\mu - \lambda_k$ and $\Lambda_{k-\pi} = -\mu + \lambda_k$ with $\lambda_k = [\mathcal{T}^2\cos^2(k) + \varepsilon^2 x^2]^{1/2}$, thus $\lambda_k = \lambda_{\pi-k}$. While $\Lambda_k < 0$ for all $k \in (0, \pi/2)$, in an interval of k the $\Lambda_{k-\pi}$-s can be positive. We characterize a given state by a wave number k_m, so that $\langle\hat{\eta}^\dagger_k\hat{\eta}_k\rangle_{k_m} = 1$ for all k and $\langle\hat{\eta}^\dagger_{k-\pi}\hat{\eta}_{k-\pi}\rangle_{k_m} = 0$ for $k \in (0, k_m)$ and 1 for $k \in (k_m, \pi/2)$. The energy per site is given by $e(k_m) = L^{-1}\sum_{k\in(0,k_m)}\Lambda_k + L^{-1}\sum_{k\in(k_m,\pi/2)}(\Lambda_k + \Lambda_{k-\pi}) + \varepsilon x^2$. Using the representation

$$\hat{x} = \frac{1}{L}\sum_{k>0}(\hat{c}^\dagger_k\hat{c}_{k-\pi} + \hat{c}^\dagger_{k-\pi}\hat{c}_k) \quad (6)$$

the self-consistency equation

$$x = \frac{\varepsilon x}{\pi}\int_0^{k_m} dk\,\frac{1}{\sqrt{\mathcal{T}^2\cos^2(k) + \varepsilon^2 x^2}} \quad (7)$$

for the expectation value x of the imbalance in the given state is derived. In the ground state $e_0 = \min_{k_m} e(k_m)$.

The self-consistency equation always has the trivial solution $x = 0$ and up to two nontrivial solutions $x \in (0, 1/2]$. The stable solution minimizes the ground state energy e_0. If x solves Eq. (7), then $-x$ is also a solution, resulting in two equivalent ground states and thus in a broken Ising symmetry. With respect to the values of k_m and x, three phases can be distinguished: Mott insulating (MI), superfluid (SF), and density wave (DW). Table I summarizes the values of k_m, the imbalance x, the density $\rho = \langle\hat{\rho}\rangle_{\text{GS}} = 1/L\sum_j\langle\hat{a}^\dagger_j\hat{a}_j\rangle_{\text{GS}}$ and energy gap Δe in the three phases. The upper bound $\tilde{k}_m$ of k_m in the SF phase is given by $\tilde{k}_m = 2\arctan[\exp(\pi\mathcal{T}/\varepsilon)] - \pi/2$ and $\mu/\mathcal{T} = 2\cos(\tilde{k}_m)$ is the metastability line in Fig. 1. As the energy

TABLE I. Characterization of the Mott insulating (MI), superfluid (SF) and density wave (DW) of the ground state phases of the Hamiltonian (4). Here x is the imbalance (3), ρ the particle density, Δe the energy gap and k_m the minimum wave number of the eigenmodes occupied in the ground state.

	MI	SF	DW
k_m	0	$\in (0, \tilde{k}_m)$	$\pi/2$
x	0	0	$\in (0, 1/2]$
ρ	1	$\in (1/2, 1)$	1/2
Δe	> 0	0	> 0

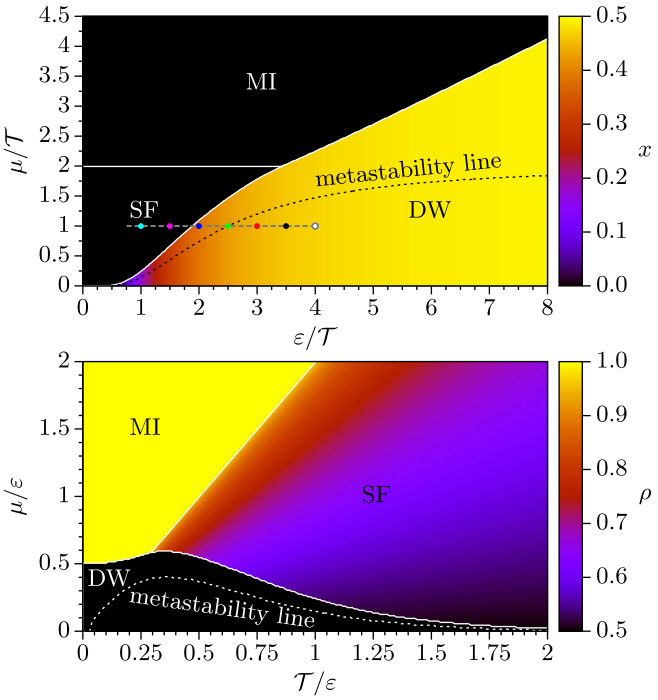

FIG. 1. Phase diagram of the Hamiltonian (4). The metastability line separates the regions with one (below) and two (above) nontrivial positive solutions of Eq. (7) for x in the DW phase. The colored dots in the upper panel indicate the end points of the DW → SF quenches shown in Fig. 2, the white dot represents the starting point. The SF → DW quenches analyzed in Fig. 4 run in the reverse direction along the same line, starting at $\varepsilon/\mathcal{T} = 0$.

gap Δe vanishes in the SF phase, the SF ground state is a critical ground state. Because of $x \neq 0$ the Ising symmetry is broken in the DW phase. Figure 1 shows the phase diagram for the Hamiltonian (4): The phase transition between the DW state and the MI state or the SF state is of first order. The value of k_m and concomitantly x and ρ display a discontinuity at the transition point. In the SF phase k_m varies continuously and the transition between the SF and the MI states is continuous. Because of the vanishing energy gap Δe in the SF phase, the SF correlation function $\langle \hat{a}^\dagger_{j+r}\hat{a}_j\rangle_{\mathrm{GS}}$ decays algebraically with the distance r, while in the DW phase the SF correlation functions decay exponentially.

Next we turn to the nonequilibrium dynamics governed by the Hamiltonian (4) and compute the time evolution of the imbalance $x(t)$ as well as the time-dependent SF correlation functions $\langle \hat{a}^\dagger_{j+r}\hat{a}_j\rangle_t$ after a sudden quench. The system is prepared in its ground state for a given set of parameters and then driven out of equilibrium by setting $(\mathcal{T}_0, \mu_0, \varepsilon_0) \to (\mathcal{T}, \mu, \varepsilon)$.

The time evolution operator $\exp(-\imath\hat{H}t)$, with $\hat{H}$ given by Eq. (4), can for infinitesimal time steps t be treated in the same way as the partition function above, resulting in an effective time-dependent Hamiltonian $\hat{H}(t)$ describing the dynamics. $\hat{H}(t)$ is identical with the Hamiltonian $\hat{H}$ from Eq. (4) but with x replaced by a time-dependent function $x(t)$ that fulfills at each time t the self-consistency equation $x(t) = \langle\psi_0|\hat{x}(t)|\psi_0\rangle$, where $\hat{x}(t)$ is the operator $\hat{x}$ from Eq. (6) in the Heisenberg picture. This also guarantees that the total energy is conserved under the time evolution, i.e., $\partial\langle\hat{H}(t)\rangle/\partial t = 0$. The representation (5) is then used to derive equations of motion for $\hat{c}^\dagger_k(t)$ and $\hat{c}^\dagger_{k-\pi}(t)$ and their Hermitian adjoints in the Heisenberg picture [45]. Expressing them in the free fermion operators that diagonalize the momentary Hamiltonian $\hat{H}(t)$ yields a system of $2L$ coupled ordinary first-order differential equations for the time-dependent Bogoliubov-parameters. Their time derivative also depends on $x(t)$, which is determined with the time-dependent version of Eq. (6) involving again the Bogoliubov parameters. The nonlinear system of ordinary differential equations is then integrated numerically using standard methods [46].

In the following we focus on quenches which change ε and keep $\mathcal{T}$ and μ constant [47]. Results for quenches starting in the DW phase decreasing ε are shown in Fig. 2: The inset shows that $x(t)$ decays quickly to a stationary value x_{stat} and is modulated by small oscillations with an amplitude that decays as $1/\sqrt{t}$. The main panel displays x_{stat} as a function of $\varepsilon/\mathcal{T}$. A dynamical phase transition occurs when x_{stat} vanishes. A numerical fit shows that it is located at

$$(\varepsilon/\mathcal{T})_{\mathrm{crit}} = \frac{2\varepsilon_0/\mathcal{T}_0}{2 + \varepsilon_0/\mathcal{T}_0}, \tag{8}$$

independent of the chemical potential μ. The exponential decay of the time-dependent SF correlation functions

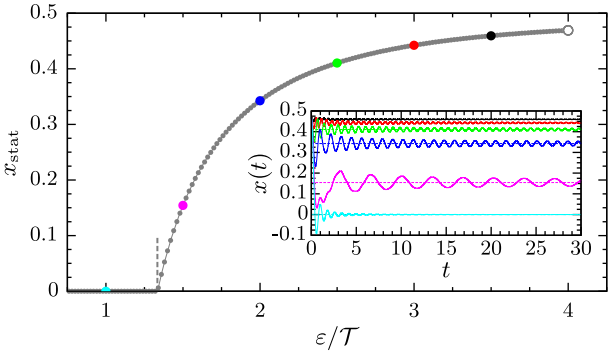

FIG. 2. Inset: Time evolution of the imbalance $x(t)$ after the quenches $(\mu_0/\mathcal{T}_0 = 1, \varepsilon_0/\mathcal{T}_0 = 4) \to (\mu/\mathcal{T} = 1, \varepsilon/\mathcal{T})$ with $\varepsilon/\mathcal{T} = 3.5$ (black), 3 (red), 2.5 (green), 2 (blue), 1.5 (pink), 1 (cyan). The broken lines indicate the values of x_{stat}. The quenches are also illustrated in the phase diagram in the upper panel of Fig. 1. Main panel: Values of the imbalance in the stationary state x_{stat} after different quench protocols $(\mu_0/\mathcal{T}_0 = 1, \varepsilon_0/\mathcal{T}_0 = 4) \to (\mu/\mathcal{T} = 1, \varepsilon/\mathcal{T})$. The vertical broken line indicates the dynamic phase transition according to Eq. (8). The white dot corresponds to "no quench" [i.e., x given by Eq. (3)] and colored points correspond to x_{stat} for the quenches shown in the inset in the same color, and to the points indicated in the upper panel of Fig. 1.

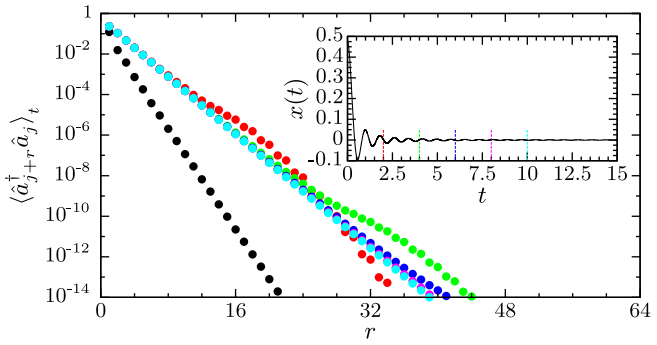

FIG. 3. Time evolution of the SF correlation function $\langle \hat{a}^\dagger_{j+r}\hat{a}_j\rangle_t$ (main panel) and the imbalance $x(t)$ (inset) after a DW → SF quench $(\mu_0/\mathcal{T}_0 = 1, \varepsilon_0/\mathcal{T}_0 = 4) \rightarrow (\mu/\mathcal{T} = 1, \varepsilon/\mathcal{T} = 1)$. Color code: $t = 0$ (black circle), 2 (red circle), 4 (green circle), 6 (blue circle), 8 (pink circle), 10 (cyan circle). The exponential decay with r is preserved under the dynamic phase transition, but the correlation length increases during the relaxation process.

$\langle \hat{a}^\dagger_{j+r}\hat{a}_j\rangle_t$, shown in Fig. 3, implies the absence of SF order after DW → SF quenches, also for $x_{\text{stat}} = 0$.

For quenches starting in the SF phase it is $x(t = 0) = 0$, which implies that $x(t) = 0$ is a solution of the self-consistency equation for all $t > 0$. In the following we test the stability of this solution adding a small perturbation x_0 to the imbalance. We find that for quenches not too deep into the DW phase $x(t)$ remains close to 0 (left inset of Fig. 4). However, for stronger quenches the value x_{max} of the maxima in the oscillations of $x(t)$ becomes much larger than the perturbation x_0 (right inset of Fig. 4) and the time-averaged imbalance is positive and independent of x_0, indicating the presence of (time-averaged) DW order. We can identify a sharp dynamical transition between a region for which the solution $x(t) = 0$ is stable and a region for which it is not stable (main panel of Fig. 4). This dynamical transition coincides with the metastability line within the DW phase and thus depends on the chemical potential in contrast to the dynamical phase transition after DW → SF quenches. Denoting the distance to the dynamic phase transition with δ, i.e., $\delta = (\varepsilon/\mathcal{T}) - (\varepsilon/\mathcal{T})_{\text{crit}}$, we find power-law dependences $x_{\text{max}} \propto \delta^{1/2}$ and $t_{\text{max}} \propto \delta^{-1/2}$ for small values of δ with x_{max} the value of the maxima of the oscillations of $x(t)$ and t_{max} the time of the first maximum of $x(t)$ after the quench.

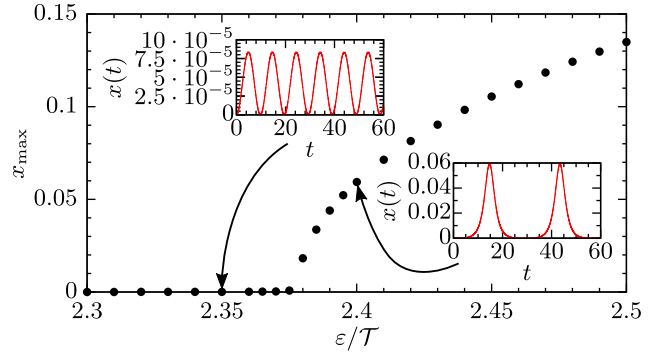

FIG. 4. Main panel: $\varepsilon/\mathcal{T}$ dependence of x_{max} in the vicinity of the dynamic phase transition for quenches with $(\mu_0/\mathcal{T}_0 = 1, \varepsilon_0/\mathcal{T}_0 = 0) \rightarrow (\mu/\mathcal{T} = 1, \varepsilon/\mathcal{T})$. The dynamic phase transition is indicated by an increase of x_{max}. Insets: Time evolution of the imbalance for the quench protocols with $\varepsilon/\mathcal{T} = 2.35$ (below the dynamic phase transition) and $\varepsilon/\mathcal{T} = 2.4$ (above the dynamic phase transition). The value of the perturbation x_0 is 10^{-6}.

For quenches from the SF phase into the DW phase across the metastability line we find that the SF correlation functions still decay algebraically, indicating the simultaneous presence of quasi-long-range SF order and (time-averaged) DW order; see Fig. 5. Consequently the system attains dynamically generated supersolid properties after strong enough quenches from the DW into the SF phase, which is not the ground state, but a high energy state. Furthermore, it is interesting to note that for times with $x(t) > 0$ there is an even-odd modulation of the SF correlation functions which increases with $x(t)$ and which disappears when the imbalance goes back to 0 (see Fig. 5). The density modulations reflect even-odd modulations of the SF correlation functions.

Thus we predict that (time-averaged) SS properties emerge during the time evolution of a SF initial state in a BH system under the influence of sufficiently strong cavity mediated long-range interactions. Superfluidity is not lost and the periodically modulated site occupation imbalance builds up beyond a critical interaction strength. The dynamical emergence of diagonal long-range DW order on top of off-diagonal (quasi)-long-range SF order is a feature of the nonequilibrium dynamics of closed

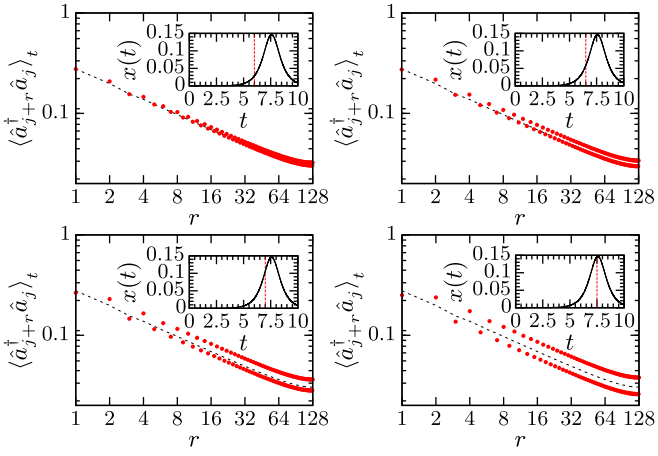

FIG. 5. Time evolution of the SF correlation function $\langle \hat{a}^\dagger_{j+r}\hat{a}_j\rangle_t$ after the quench $(\mu_0/\mathcal{T}_0 = 1, \varepsilon_0/\mathcal{T}_0 = 0) \rightarrow (\mu/\mathcal{T} = 1, \varepsilon/\mathcal{T} = 2.5)$ from the SF into the DW phase. The algebraic decay of the SF correlation function in the initial SF ground state (scattered black line) is preserved under the dynamic phase transition, but for $x(t) > 0$ the curve splits up into two curves for even and odd distances between the spins.

quantum system that has to our knowledge never been reported before. Since its origin is the presence of the global range interactions we expect it to be robust and to be observable also in two- and three-dimensional BH systems with cavity-induced interactions, for hard-core as well as soft-core bosons. It would be interesting to check these predictions with, for instance, tVMC methods [40].

It is also interesting to note that the system we analyzed does not thermalize for some quenches: the high energy states that dynamically generate SS order after some SF → DW quenches cannot be described by a finite temperature equilibrium ensemble, since the considered system does not display SS equilibrium phases, neither in the ground state (cf. Fig. 1) nor at finite temperatures. This is particularly remarkable considering the fact that for finite size (finite L) the system is nonintegrable. Integrability is only achieved by the method that we use to handle the coupling of (the cavity induced) long-range interactions and the short-range interactions in the thermodynamic limit, which opens a way to solve exactly other Hamiltonians with long-range and short-range interactions as well, ranging from bosons in external potentials over magnetic systems to fermionic systems.

Our predictions of remanent, metastable DW order after DW → SF quenches and the dynamical generation of periodically modulated DW order superposed to metastable SF order after SF → DW quenches can be tested experimentally in a cavity setup like the one used in Ref. [9], even though this setup is two-dimensional and involves soft-core bosons. Preliminary experimental indications for such metastability phenomena occurring after quenches of the cavity induced interaction strength have indeed been reported recently [48] and our exact results will serve as a firm reference for the interpretation and understanding of such experiments.

This work was supported by the National Research Fund, Grants No. K109577, No. K115959 and No. KKP-126749. H. R. extends thanks to the "Theoretical Physics Workshop" and F. I. and G. R. to the Saarland University for supporting their visits to Budapest and Saarbrücken, respectively.

*bebla@lusi.uni-sb.de
†h.rieger@physik.uni-saarland.de
‡roosz.gergo@wigner.mta.hu
§igloi.ferenc@wigner.mta.hu

[1] For a review see, I. Bloch, J. Dalibard, and W. Zwerger, Rev. Mod. Phys. **80**, 885 (2008).
[2] A. Eckardt, Rev. Mod. Phys. **89**, 011004 (2017).
[3] H. Gersch and G. Knollman, Phys. Rev. **129**, 959 (1963).
[4] M. P. A. Fisher, P. B. Weichman, G. Grinstein, and D. S. Fisher, Phys. Rev. B **40**, 546 (1989).
[5] M. Lewenstein, A. Sanpera, V. Ahufinger, B. Damski, A. Sen(De), and U. Sen, Adv. Phys. **56**, 243 (2007).
[6] D. Jaksch and P. Zoller, Ann. Phys. (Amsterdam) **315**, 52 (2005).
[7] R. Mottl, F. Brennecke, K. Baumann, R. Landig, T. Donner, and T. Esslinger, Science **336**, 1570 (2012).
[8] J. Klinder, H. Keßler, M. R. Bakhtiari, M. Thorwart, and A. Hemmerich, Phys. Rev. Lett. **115**, 230403 (2015).
[9] R. Landig, L. Hruby, N. Dogra, M. Landini, R. Mottl, T. Donner, and T. Esslinger, Nature (London) **532**, 476 (2016).
[10] Y. Chen, Z. Yu, and H. Zhai, Phys. Rev. A **93**, 041601(R) (2016).
[11] N. Dogra, F. Brennecke, S. D. Huber, and T. Donner, Phys. Rev. A **94**, 023632 (2016).
[12] A. E. Niederle, G. Morigi, and H. Rieger, Phys. Rev. A **94**, 033607 (2016).
[13] B. Sundar and E. J. Mueller, Phys. Rev. A **94**, 033631 (2016).
[14] J. Panas, A. Kauch, and K. Byczuk, Phys. Rev. B **95**, 115105 (2017).
[15] T. Flottat, L. de Forges de Parny, F. Hébert, V. G. Rousseau, and G. G. Batrouni, Phys. Rev. B **95**, 144501 (2017).
[16] A. Polkovnikov, K. Sengupta, A. Silva, and M. Vengalattore, Rev. Mod. Phys. **83**, 863 (2011).
[17] M. Rigol, V. Dunjko, V. Yurovsky, and M. Olshanii, Phys. Rev. Lett. **98**, 050405 (2007); M. Rigol, V. Dunjko, and M. Olshanii, Nature (London) **452**, 854 (2008).
[18] P. Calabrese and J. Cardy, Phys. Rev. Lett. **96**, 136801 (2006).
[19] P. Calabrese and J. Cardy, J. Stat. Mech. (2007) P06008.
[20] M. A. Cazalilla, Phys. Rev. Lett. **97**, 156403 (2006); A. Iucci and M. A. Cazalilla, New J. Phys. **12**, 055019 (2010); A. Iucci and M. A. Cazalilla, Phys. Rev. A **80**, 063619 (2009).
[21] S. R. Manmana, S. Wessel, R. M. Noack, and A. Muramatsu, Phys. Rev. Lett. **98**, 210405 (2007).
[22] M. Cramer, C. M. Dawson, J. Eisert, and T. J. Osborne, Phys. Rev. Lett. **100**, 030602 (2008); M. Cramer and J. Eisert, New J. Phys. **12**, 055020 (2010); M. Cramer, A. Flesch, I. P. McCulloch, U. Schollwöck, and J. Eisert, Phys. Rev. Lett. **101**, 063001 (2008); A. Flesch, M. Cramer, I. P. McCulloch, U. Schollwöck, and J. Eisert, Phys. Rev. A **78**, 033608 (2008).
[23] T. Barthel and U. Schollwöck, Phys. Rev. Lett. **100**, 100601 (2008).
[24] M. Kollar and M. Eckstein, Phys. Rev. A **78**, 013626 (2008).
[25] S. Sotiriadis, P. Calabrese, and J. Cardy, Europhys. Lett. **87**, 20002 (2009).
[26] G. Roux, Phys. Rev. A **79**, 021608 (2009); **81**, 053604 (2010).
[27] S. Sotiriadis, D. Fioretto, and G. Mussardo, J. Stat. Mech. (2012) P02017; D. Fioretto and G. Mussardo, New J. Phys. **12**, 055015 (2010); G. P. Brandino, A. De Luca, R. M. Konik, and G. Mussardo, Phys. Rev. B **85**, 214435 (2012).
[28] B. Wouters, J. De Nardis, M. Brockmann, D. Fioretto, M. Rigol, and J.-S. Caux, Phys. Rev. Lett. **113**, 117202 (2014).
[29] B. Pozsgay, M. Mestyán, M. A. Werner, M. Kormos, G. Zaránd, and G. Takács, Phys. Rev. Lett. **113**, 117203 (2014).
[30] G. Goldstein and N. Andrei, Phys. Rev. A **90**, 043625 (2014).
[31] B. Pozsgay, J. Stat. Mech. (2014) P09026.
[32] B. Pozsgay, J. Stat. Mech. (2014) P10045.
[33] F. H. L. Essler, G. Mussardo, and M. Panfil, Phys. Rev. A **91**, 051602 (2015).

[34] E. Ilievski, J. De Nardis, B. Wouters, J.-S. Caux, F. H. L. Essler, and T. Prosen, Phys. Rev. Lett. **115**, 157201 (2015).
[35] E. Ilievski, M. Medenjak, T. Prosen, and L. Zadnik, J. Stat. Mech. (2016) 064008.
[36] B. Doyon, Commun. Math. Phys. **351**, 155 (2017).
[37] T. Stöferle, H. Moritz, C. Schori, M. Köhl, and T. Esslinger, Phys. Rev. Lett. **92**, 130403 (2004); T. Kinoshita, T. Wenger, and D. S. Weiss, Science **305**, 1125 (2004); L. Fallani, J. E. Lye, V. Guarrera, C. Fort, and M. Inguscio, Phys. Rev. Lett. **98**, 130404 (2007); N. Gemelke, X. Zhang, C. L. Hung, and C. Chin, Nature **460**, 995 (2009); I. Bloch, J. Dalibard, and S. Nascimbene, Nat. Phys. **8**, 267 (2012).
[38] A. J. Daley, H. Pichler, J. Schachenmayer, and P. Zoller, Phys. Rev. Lett. **109**, 020505 (2012).
[39] C. Kollath, A. M. Läuchli, and E. Altman, Phys. Rev. Lett. **98**, 180601 (2007); G. Biroli, C. Kollath, and A. M. Läuchli, Phys. Rev. Lett. **105**, 250401 (2010).
[40] G. Carleo, F. Becca, M. Schiró, and M. Fabrizio, Sci. Rep. **2**, 243 (2012); G. Carleo, F. Becca, L. Sanchez-Palencia, S. Sorella, and M. Fabrizio, Phys. Rev. A **89**, 031602(R) (2014).
[41] H. U. R. Strand, M. Eckstein, and P. Werner, Phys. Rev. X **5**, 011038 (2015).
[42] C. Maschler and H. Ritsch, Phys. Rev. Lett. **95**, 260401 (2005); J. Larson, B. Damski, G. Morigi, and M. Lewenstein, Phys. Rev. Lett. **100**, 050401 (2008); S. Fernández-Vidal, G. De Chiara, J. Larson, and G. Morigi, Phys. Rev. A **81**, 043407 (2010).
[43] H. Habibian, A. Winter, S. Paganelli, H. Rieger, and G. Morigi, Phys. Rev. Lett. **110**, 075304 (2013); H. Habibian, A. Winter, S. Paganelli, H. Rieger, and G. Morigi, Phys. Rev. A **88**, 043618 (2013).
[44] For a similar treatment of a classical system with global-range interactions see M. Kardar, Phys. Rev. B **28**, 244 (1983).
[45] F. Iglói, B. Blass, G. Roósz, and H. Rieger, arXiv: 1808.01993.
[46] We used $L = 256$ and $L = 512$ and checked that the results we show do not depend on system size for the times we considered.
[47] Since the term $-\mu L\hat{\rho}$ commutes with $H(t)$ quenches changing only the chemical potential leave the system in an eigenstate of $H(t)$, not necessarily the ground state, and the time evolution is trivial.
[48] L. Hruby, N. Dogra, M. Landini, T. Donner, and T. Esslinger, Proc. Natl. Acad. Sci. U.S.A. **115**, 3279 (2018).